Amperometric Transduction and Amplification of Optical Signals Recorded by a Phenoxynaphthacenequinone Monolayer Electrode: Photochemical and pH-Gated Electron Transfer

Amihood Doron, Moshe Portnoy, Mazzi Lion-Dagan, Eugenii Katz, and Itamar Willner*

Contribution from the Institute of Chemistry and The Farkas Center for Light-Induced Processes, The Hebrew University of Jerusalem, Jerusalem 91904, Israel

Received May 30, 1996[⊗]

Abstract: A phenoxynaphthacenequinone photoisomerizable monolayer was assembled onto an Au electrode. The resulting "*trans*"-quinone monolayer exhibits poor electrochemical reversibility due to a nondensely-packed configuration. Treatment of the *trans*-quinone monolayer with 1-tetradecanethiol yields a densely-packed monolayer that exhibits electrochemical reversibility. The electrochemical response of the *trans*-quinone monolayer electrode is pH-dependent, consistent with a two-electron and two-proton redox process. Photoisomerization of the *trans*-quinone monolayer (305 nm $< \lambda <$ 320 nm) generates the *ana*-quinone monolayer that lacks electrochemical activity. Upon photoisomerization of the *ana*-quinone monolayer to the *trans*-quinone state ($\lambda >$ 430 nm), the electroactivity of the monolayer is restored. By cyclic photoisomerization of the electrode between the *ana*- and *trans*-quinone states, reversible amperometric transduction of the recorded optical signals was accomplished. Coupling of redox-active materials, such as $Fe(CN)_6^{3-}$ or *N,N′*-dibenzyl-4,4′-bipyridinium (BV^{2+}) to the photoisomerizable electroactive monolayer electrode allows vectorial electron transfer and amplification of the electrical response of the *trans*-quinone monolayer by the electrocatalyzed reduction of $Fe(CN)_6^{3-}$ or BV^{2+}. The vectorial electron transfer from the *trans*-quinone monolayer to BV^{2+} is gated by the pH of the medium. The *trans*-quinone monolayer electrode was coupled to the redox mediator BV^{2+} and the enzyme nitrate reductase. In the presence of NO_3^-, the multicomponent system in the *trans*-quinone state leads to the bioelectrocatalyzed reduction of nitrate and the transduction of an amplified cathodic current. In this system, the vectorial reduction of BV^{2+} to $BV^{+\bullet}$ yields an electron mediator that activates the biocatalyzed process. By cyclic photoisomerization of the monolayer between the *ana*- and *trans*-quinone states, reversible light-induced activation and deactivation of the vectorial electron transfer in the system is accomplished. The functionalized electrode assemblies provide a means for the amplified amperometric transduction of recorded optical signals.

Introduction

The development of molecular electronic and optoelectronic systems represents a rapidly progressing research field aimed to duplicate functions of bulk electronic and optical devices at the molecular level and to tailor molecular-scale electronic devices.[1,2] In molecular electronic and optoelectronic devices, an external signal triggers-on a chemical functionality that is transduced as a physical output. The design of molecular electronic and optoelectronic devices requires the organization of chemical assemblies of signal-switchable functionalities and their integration with appropriate supports that allow the electronic or optical transduction of the activated chemical functionality.

Optical,[3] electrochemical,[4] thermal,[5] and pH[6] signals have been used to activate switchable molecular functions. Electrochemically-induced translocation of molecular components in supramolecular complexes were reported as electroactivated molecular switches.[7] Light-controlled association and dissociation of ions to and from photoisomerizable molecular receptors,[8] complexation of metalloporphyrins with photoisomerizable ligands,[9] and activation of light-driven active transport[10] of ions,

[⊗] Abstract published in *Advance ACS Abstracts,* September 1, 1996.

(1) (a) Fabbrizzi, L.; Poggi, A. *Chem. Soc. Rev.* **1995**, *24*, 197. (b) Carter, F. L.; Schultz, A.; Duckworth, D. In *Molecular Electronic Devices II;* Carter, F. L., Ed.; Dekker: New York, 1987, p 183.

(2) (a) Willner, I.; Willner, B. In *Bioorganic Photochemistry−Biological Application of Photochemical Switches;* Morrison, H., Ed.; Wiley: New York, 1993; Vol. 2, p 1. (b) Willner, I.; Rubin, S. *Angew. Chem., Int. Ed. Engl.* **1996**, *35*, 367. (c) Willner, I.; Willner, B. *Adv. Mater.* **1995**, *7*, 587. (d) Willner, I.; Willner, B. *Pure Appl. Chem.* **1996**. In press.

(3) (a) Parthenopoulos, D. A.; Rentzepis, P. M. *Science* **1989**, *245*, 843. (b) Stauffer, M. T.; Grosko, J. A.; Ismail, K. Z.; Weber, S. G. *J. Chem. Soc., Chem. Commun.* **1995**, 1695. (c) Huck, N. P. M.; Feringa, B. L. *J. Chem. Soc., Chem. Commun.* **1995**, 1095.

(4) (a) Liu, Z.; Hashimoto, K.; Fujishima, A. *Nature* **1990**, *347*, 658. (b) Morigaki, K.; Liu, Z.; Hashimoto, K.; Fujishima, A. *J. Phys. Chem.* **1995**, *99*, 14771. (c) Gallardo, B. S.; Hwa, M. J.; Abbott, N. L. *Langmuir* **1995**, *11*, 4209.

(5) (a) Katz, E.; Willner, I. *Electroanalysis* **1995**, *7*, 417. (b) Moriguchi, I.; Hanai, K.; Hoshikuma, A.; Teraoka, Y.; Kagawa, S. *Chem. Lett.* **1994**, 691.

(6) (a) Katz, E.; Lion-Dagan, M.; Willner, I. *J. Electroanal. Chem.* **1996**, *408*, 107. (b) Katz, E.; de Lacey, A. L.; Fernandez, V. M. *J. Electroanal. Chem.* **1993**, *358*, 261. (c) Nakashima, N.; Taguchi, T. *Colloids Surf., A* **1995**, *103*, 159.

(7) Bissell, R. A.; Córdova, E.; Kaifer, A. E.; Stoddart, J. F. *Nature* **1994**, *369*, 133.

(8) (a) De Santis, G.; Fabbrizzi, L.; Licchelli, M.; Pallavicini, P.; Perotti, A.; Poggi, A. *Supramol. Chem.* **1994**, *3*, 115. (b) Singewald, E. T.; Mirkin, C. A.; Stern, C. L. *Angew. Chem., Int. Ed. Engl.* **1995**, *34*, 1624. (c) Winkler, J. D.; Deshayes, K.; Shao, B. In *Bioorganic Photochemistry-Biological Application of Photochemical Switches*; Morrison, H., Ed.; Wiley: New York 1993; Vol. 2, p 169. (d) Rahman, S. M. F.; Fukunishi, K. *J. Chem. Soc., Chem. Commun.* **1994**, 917. (e) Blank, M.; Soo, L. M.; Wassermann, N. H.; Erlanger, B. F. *Science* **1981**, *214*, 70. (f) Shinkai, S.; Shigematsu, K.; Sato, M.; Manabe, O. *J. Chem. Soc., Perkin Trans. 1* **1982**, 2735. (g) Shinkai, S.; Kouno, T.; Kusano, Y.; Manabe, O. *J. Chem. Soc., Perkin Trans. 1* **1982**, 2741.

(9) Iseki, Y.; Inoue, S. *J. Chem. Soc., Chem. Commun.* **1994**, 2577.

(10) (a) Higuchi, M.; Takizawa, A.; Kinoshita, T.; Tsujita, Y. *Macromolecules* **1987**, *20*, 2888. (b) Shinkai, S.; Shigematsu, K.; Ogawa, T.; Minami, T.; Manabe, O. *Tetrahedron Lett.* **1980**, *21*, 4463. (c) Shinkai, S.; Minami, T.; Kusano, T.; Manabe, O. *J. Am. Chem. Soc.* **1982**, *104*, 1967.

S0002-7863(96)01814-8 CCC: $12.00

or formation and dissociation of H-bonded photoisomerizable supramolecular complexes,[11] represent optical activation of molecular recognition phenomena. Similarly, light-regulated formation and dissociation of donor−acceptor supramolecular complexes[12] (i.e., association of *cis*-azobenzene-4,4′-bipyridinium electron acceptor to eosin acting as electron donor and dissociation of the complex with the *trans*-azobenzene-4,4′-bipyridinium electron acceptor) represents an optical molecular switch. Light-triggered conformational changes of photoisomerizable polymers[13] or photoisomerizable polypeptides[14] demonstrate optically-activated structural functions of macromolecules.

Physical transduction of the switchable function allows the application of the molecular assembly as a "write" and "read" memory device. Amperometric transduction of recorded optical signals provides a general method to tailor molecular optoelectronic devices. By this approach, the recorded optical signal triggers-on a chemical transformation resulting in an electroactive entity that permits the transduction of the recorded information upon integration with an electrode surface. Dihydroxy-bis-thiophene ethene was recently reported as a molecular optical memory, exhibiting write−read−store functions.[15] The electrochemical activity of its 6π-photocyclized isomer allows the amperometric read-out of the optical information, and its oxidized quinoid product stores the recorded photonic information. Amperometric or piezoelectric transduction of recorded optical signals was recently achieved by the functionalization of electrodes with monolayers. For example, an eosin monolayer assembled on an electrode forms light-triggered supramolecular electroactive complexes with a *cis*-azobenzene-4,4′-bipyridinium electron acceptor.[16] Light-induced formation of the supramolecular complex at the electrode surface allows the amperometric or piezoelectric transduction of the recorded optical signals.

Amplified amperometric transduction of recorded optical signals was accomplished by light-induced activation and deactivation of redox enzymes,[17] or other photoswitchable biomaterials.[18] In these systems, the recorded light signal is electrically amplified by the optically-stimulated redox transformation of the biocatalyst. Three different approaches were employed to reversibly activate redox proteins. In the first approach, the electrode is modified by a photoisomerizable monolayer that acts as a photoactive command surface,[19] particularly for the association or dissociation of the redox protein from the electrode interface.[20,21] Optical signals recorded by the monolayer then control the resulting electrical communication between the redox protein and the electrode surface. Amplified amperometric transduction of optical signals in the presence of photoisomerizable electrode was accomplished by coupling the cytochrome *c*/cytochrome oxidase[20] or glucose oxidase[21] redox catalysts to the functionalized electrodes. A second method to photostimulate redox enzymes coupled to electrode surface involved the application of photoisomerizable electron mediators as optical triggers for the bioelectrocatalytic transformations.[22] The third approach to photostimulate biocatalysts included the chemical modification of redox enzymes by photoisomerizable components and immobilization of the photoswitchable biocatalysts onto electrode surfaces.[23,24]

Photoisomerization of organic compounds was extensively studied with the general context of photochromic substrates.[25] Development of photoisomerizable quinoid compounds provides a means for the electrochemical transduction of the recorded light signal via the electroactive quinoid moiety. Phenoxynaphthacenequinone reveals reversible photoisomerizable features, and the "*trans*"-quinone state undergoes photochemical rearrangement to the "*ana*"-quinone state.[26] In a recent preliminary study,[27] we reported on the organization of a photoisomerizable phenoxynaphthacenequinone monolayer electrode as an active interface for the electrochemical transduction of recorded optical signals. Here we present the comprehensive characterization of the system and discuss various means to amplify the transduced currents.

Experimental Section

Materials. 6-[(4-Carboxymethyl)phenyl)oxy]-5,12-naphthacenequinone potassium salt (**2a**) was synthesized according to the recently reported method.[26e] For **2a**: mp 220−224 °C (dec); ^{1}H NMR (200 MHz, $CDCl_3$) δ(ppm) 3.4 (s, 2H), 6.78 (d, J = 7.3 Hz, 2H), 7.13 (d, J = 7.3 Hz, 2H), 7.70−7.94 (m, 4H), 8.07 (dm, J = 7 Hz, 2H), 8.23 (m, 1H), 8.40 (d, J = 7.5 Hz, 1H), 8.84 (s, 1H). Anal. Calcd: C, 69.96; H, 3.36. Found: C, 70.26; H, 3.60. The "*ana*"-quinone state **2b** was produced photochemically; conversion of **2a** to **2b** in a DMSO solution corresponds to ca. 70%. The absorbance maxima in dry dimethylsulfoxide was found to be the following: **2a**, *trans*-state, λ = 245 and 398 nm; **2b**, *ana*-state, λ = 483, 452, and 248 nm.

(11) (a) Rosengaus, J.; Willner, I. *J. Chem. Soc., Chem. Commun.* **1993**, 1044. (b) Rosengaus, J.; Willner, I. *J. Phys. Org. Chem.* **1995**, *8*, 54. (c) Würthner, F.; Rebek, J., Jr. *Angew. Chem., Int. Ed. Engl.* **1995**, *34*, 446.

(12) Willner, I.; Marx, S.; Eichen, Y. *Angew. Chem., Int. Ed. Engl.* **1992**, *31*, 1243.

(13) (a) Ishihara, K.; Okazaki, A.; Negishi, N.; Shinohara, I.; Okano, T.; Kataoka, K.; Sakurai, Y. *J. Appl. Polym. Sci.* **1982**, *27*, 239. (b) Irie, M. *Adv. Polym. Sci.* **1990**, *94*, 27.

(14) (a) Pieroni, O.; Fissi, A. *J. Photochem. Photobiol., B* **1992**, *12*, 125. (b) Malcolm, B. R.; Pieroni, O. *Biopolymers* **1990**, *29*, 1121.

(15) (a) Kawai, S. H.; Gilat, S. L.; Lehn, J.-M. *J. Chem. Soc., Chem. Commun.* **1994**, 1011. (b) Gilat, S. L.; Kawai, S. H.; Lehn, J.-M. *Chem. Eur. J.* **1995**, *1*, 275. (c) Kawai, S. H.; Gilat, S. L.; Ponsinet, R.; Lehn, J.-M. *Chem. Eur. J.* **1995**, *1*, 285.

(16) Marx-Tibbon, S.; Ben-Dov, I.; Willner, I. *J. Am. Chem. Soc.* **1996**, *118*, 4717.

(17) (a) Montagnoli, G.; Monti, S.; Nannicini, L.; Felicioli, R. *Photochem. Photobiol.* **1976**, *23*, 29. (b) Aizawa, M.; Namba, K.; Suzuki, S. *Arch. Biochem. Biophys.* **1977**, *182*, 305. (c) Willner, I.; Rubin, S.; Riklin, A. *J. Am. Chem. Soc.* **1991**, *113*, 3321. (d) Willner, I.; Lion-Dagan, M.; Rubin, S.; Wönner, J.; Effenberger, F.; Bäuerle, P. *Photochem. Photobiol.* **1994**, *59*, 491.

(18) (a) Harada, M.; Sisido, M.; Hirose, J.; Nakanishi, M. *FEBS Lett.* **1991**, *286*, 6. (b) Willner, I.; Rubin, S.; Wönner, J.; Effenberger, F.; Bäuerle, P. *J. Am. Chem. Soc.* **1992**, *114*, 3150. (c) Willner, I.; Blonder, R.; Dagan, A. *J. Am. Chem. Soc.* **1994**, *116*, 9365. (d) Blonder, R.; Ben-Dov, I.; Dagan, A.; Willner, I. *Biosens. Bioelectron.* **1996**. In press.

(19) Katz, E.; Lion-Dagan, M.; Willner, I. *J. Electroanal. Chem.* **1995**, *382*, 25.

(20) (a) Lion-Dagan, M.; Katz, E.; Willner, I. *J. Chem. Soc., Chem. Commun.* **1994**, 2741. (b) Willner, I.; Lion-Dagan, M.; Marx-Tibbon, S.; Katz, E. *J. Am. Chem. Soc.* **1995**, *117*, 6581.

(21) Willner, I.; Doron, A.; Katz, E.; Levi, S.; Frank, A. J. *Langmuir* **1996**, *12*, 946.

(22) Lion-Dagan, M.; Marx-Tibbon, S.; Katz, E.; Willner, I. *Angew. Chem., Int. Ed. Engl.* **1995**, *34*, 1604.

(23) (a) Lion-Dagan, M.; Katz, E.; Willner, I. *J. Am. Chem. Soc.* **1994**, *116*, 7913. (b) Willner, I.; Lion-Dagan, M.; Katz, E. *J. Chem. Soc., Chem. Commun.* **1996**, 623.

(24) Willner, I.; Blonder, R.; Katz, E.; Stocker, A.; Bückmann, A. F. *J. Am. Chem. Soc.* **1996**, *118*, 5310.

(25) *Photochromism. Molecules and Systems*; Dürr, H., Bouas-Laurent, H., Eds.; Elsevier: London, 1990.

(26) (a) Gritsan, N. P.; Klimenko, L. S. *J. Photochem. Photobiol., A* **1993**, *70*, 103. (b) Gerasimenko, Y. E.; Parshutkin, A. A.; Poteleschenko, N. T.; Poteleschenko, V. P.; Romanov, V. V. *Zh. Prikl. Spectrosk.* **1979**, *30*, 954 (in Russian). (c) Gerasimenko, Y. E.; Poteleschenko, N. T. *Zh. Org. Khim.* **1971**, *7*, 2412 (in Russian). (d) Zelichenok, A.; Buchholtz, F.; Fischer, E.; Ratner, J.; Krongauz, V.; Anneser, H.; Bräuchle, C. *J. Photochem. Photobiol., A* **1993**, *76*, 135. (e) Buchholtz, F.; Zelichenok, A.; Krongauz, V. *Macromolecules* **1993**, *26*, 906. (f) Fang, Z.; Wang, S.; Yang, Z.; Chen, B.; Li, F.; Wang, J.; Xu, S.; Jiang, Z.; Fang, T. *J. Photochem. Photobiol., A* **1995**, *88*, 23.

(27) Doron, A.; Katz, E.; Portnoy, M.; Willner, I. *Angew. Chem., Int. Ed. Engl.* **1996**, *35*, 1535.

Nitrate reductase from *Aspergillus* sp., EC 1.6.6.2. (Boehringer, Mannheim), and all other chemicals (Aldrich, Sigma, Fluka) were used as supplied without additional purification. Ultrapure water from a Nanopure (Barnstead) source was used throughout this work.

Instruments and Methods. Absorption spectra were recorded on a Uvicon-860 (Kontron) spectrophotometer. NMR spectra were recorded with a Bruker AMX 400 or a Bruker WP-200 spectrometer. Chemical shifts were referenced to TMS and coupling constants are reported in hertz.

Electrochemical measurements were performed using a potentiostat (EG&G VersaStat) connected to a personal computer (EG&G research electrochemistry software model 270/250). The measurements were done at room temperature (ca. 25 °C) in a three-compartment electrochemical cell consisting of a chemically-modified electrode as a working electrode, a glassy carbon auxiliary electrode isolated by a glass frit, and a saturated calomel electrode (SCE) connected to the working volume with a Luggin capillary. All potentials were reported with respect to this reference electrode. Argon bubbling was used to remove oxygen from the solution in the electrochemical cell. The background solution (0.01 M phosphate buffer, pH 7.0, and 0.1 M Na_2SO_4) was used for the measurements (unless otherwise indicated). Some measurements were performed in 0.05 M Britton−Robinson buffer titrated with HCl or KOH directly in the electrochemical cell to obtain the required pH values in a broad region.

Isomerization of monolayers was achieved by subjecting the electrodes to irradiation at appropriate wavelengths. The electrodes were illuminated in the air outside the electrochemical cell. A 150 W xenon arc lamp equipped with a Schott filter ($\lambda > 430$ nm) and an IR $CuSO_4$ filter was used as the light source for generation of the "*trans*"-quinone state. An 18 W mercury pencil lamp source (Oriel-6042) with a long-wave filter (305 nm $< \lambda <$ 320 nm) was used to generate the *ana*-quinone state. The electrodes were protected from room light during the electrochemical measurements.

Electrodes and Their Modification. An Au electrode (0.5 mm diameter Au wire, geometrical area ca. 0.2 cm^2, roughness factor ca. 1.2) was used for the modifications. The Au electrodes were cleaned by boiling in 2 M KOH for 1 h followed by rinsing with water. The electrodes were stored in concentrated sulfuric acid. Prior to modification, the electrodes were rinsed with water, soaked for 10 min in concentrated nitric acid, and rinsed again with water. A cyclic voltammogram recorded in 1 M H_2SO_4 was used to determine the purity and roughness of the electrode surface just before modification.[28] An Au electrode was soaked in a solution of 0.05 M cystamine (2,2′-dithiobisethanamine, Aldrich) in water for 1 h. The electrode was then rinsed thoroughly with water to remove the physically-adsorbed cystamine. The cystamine-modified Au electrode was incubated for 1 h in ca. 0.5 mM solution of **2a** in 0.01 M HEPES aqueous/ethanolic (1:1 v/v) buffer, pH 7.3, in the presence of 10 mM 1-ethyl-3-(3-dimethylaminopropyl)carbodiimide (EDC, Aldrich). For further modification, the **2a**-modified electrode was treated with 1 mM 1-tetradecanethiol (Fluka) in ethanol for 30 min (unless otherwise indicated) and rinsed with ethanol.

Results and Discussion

The photochemistry of phenoxynaphthacenequinone was recently examined in solution.[26] The *trans*-quinone **1a** undergoes, upon UV irradiation, isomerization to the *ana*-quinone isomer **1b**. Visible light illumination of **1b** ($\lambda > 430$ nm) restores the *trans*-quinone state **1a**, (Scheme 1). The electrochemical features of the *trans*-quinone **1a**, and *ana*-quinone, **1b**, should differ substantially due to their significantly different isomeric structures. Thus, functionalization of electrode surfaces by naphthacenequinone, could yield photoactive command surfaces for the amperometric transduction of recorded optical signals. 6-[(4-Carboxymethyl)phenyl)oxy]-5,12-naphthacenequinone (**2a**) was synthesized. This compound includes the photoelectrochemical features for electrochemical transduction of recorded optical signals and the carboxylic acid chemical functionality that enables its covalent attachment to the electrode. The *trans*-quinone **2a**, was assembled on an Au electrode as shown in Scheme 2. A primary cystamine monolayer was assembled on the Au surface and **2a** was coupled to this base monolayer, as recently demonstrated for some other carboxylic acid quinone derivatives.[29] Figure 1 (curve a) shows the cyclic voltammogram of the resulting *trans*-quinone monolayer electrode. An ill-defined redox wave is observed for the *trans*-quinone monolayer. This ill-defined redox wave is attributed to the formation of a nondensely-packed quinone monolayer, where some quinone molecules are in nonelectrochemically active positions as reported recently for monolayers of quinones[30] and some other redox materials.[31] The different electroactivities of the monolayer components yield the broad ill-defined redox-wave. Organization of the densely-packed *trans*-quinone monolayer is possible by treatment of the electrode with a long-chain thiol. This cosubstrate associates to the surface pinhole defects, and its organization as a densely-packed monolayer is anticipated to stretch and align the *trans*-quinone component.[29d,31] Figure 1 (curves b−e) shows the cyclic voltammograms of the *trans*-quinone monolayer electrode at time intervals of treatment with 1-tetradecanethiol ($C_{14}SH$). The cyclic voltammogram of the *trans*-quinone becomes sharper upon treatment with $C_{14}SH$, and after 30 min of interaction with the long-chain thiol, a quasi-reversible cyclic voltammogram of constant shape is observed (Figure 1, curve e). This quasi-reversible redox wave, $E^\circ = -0.62$ V (at pH = 7.0), is attributed to the two-electron redox process of the *trans*-quinone in a densely-packed, aligned configuration of the monolayer assembly. By integration of the charge associated with the reduction (or oxidation) of the *trans*-quinone component, and assuming that its redox processes involve two electrons (vide infra), the surface density of the quinone on the electrode is estimated to be ca. 2×10^{-10} mol cm^{-2}. Figure 2 shows the cyclic voltammograms of the *trans*-quinone electroactive component in the densely-packed assembly with $C_{14}SH$ at different scan rates. The anodic current linearly depends on the scan rate (Figure 2, inset), implying that the *trans*-quinone is a surface-confined electroactive molecule. From the peak-to-peak separation of the redox waves at different scan rates (Figure 3) and by the application of Laviron's theory,[32] the electron transfer

Scheme 1. Photoisomerizable Phenoxynaphthacenequinone Derivatives

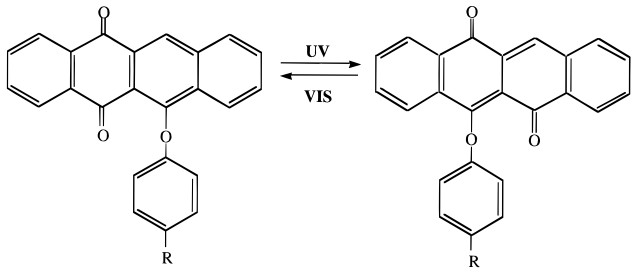

1a or **2a** "trans" **1b** or **2b** "ana"

1a,b R = H

2a,b R = CH_2CO_2H

(28) Woods, R. In *Electroanalytical Chemistry*; Bard, A. J., Ed.; Marcel Dekker: New York, 1976; Vol. 9, p 1.

(29) (a) Katz, E.; Solov'ev, A. A. *J. Electroanal. Chem.* **1990**, *291*, 171. (b) Katz, E.; Riklin, A.; Willner, I. *J. Electroanal. Chem.* **1993**, *354*, 129. (c) Katz, E.; Schlereth, D. D.; Schmidt, H.-L. *J. Electroanal. Chem.* **1994**, *367*, 59. (d) Katz, E.; Schmidt, H. L. *J. Electroanal. Chem.* **1994**, *368*, 87.

(30) (a) Sharp, M. *Electrochim. Acta* **1978**, *23*, 287. (b) Soriaga, M. P.; Stickney, J. L.; Hubbard, A. T. *J. Electroanal. Chem.* **1983**, *144*, 207. (c) Hubbard, A. T. *Heterog. Chem. Rev.* **1994**, *1*, 3.

(31) (a) Katz, E.; Itzhak, N.; Willner, I. *J. Electroanal. Chem.* **1992**, *336*, 357. (b) Katz, E.; Itzhak, N.; Willner, I. *Langmuir* **1993**, *9*, 1392.

(32) Laviron, E. *J. Electroanal. Chem.* **1979**, *101*, 19.

Scheme 2. Assembly of the Phenoxynaphthacenequinone/C_{14}SH Mixed Monolayer on an Au Electrode and Its Photoisomerization

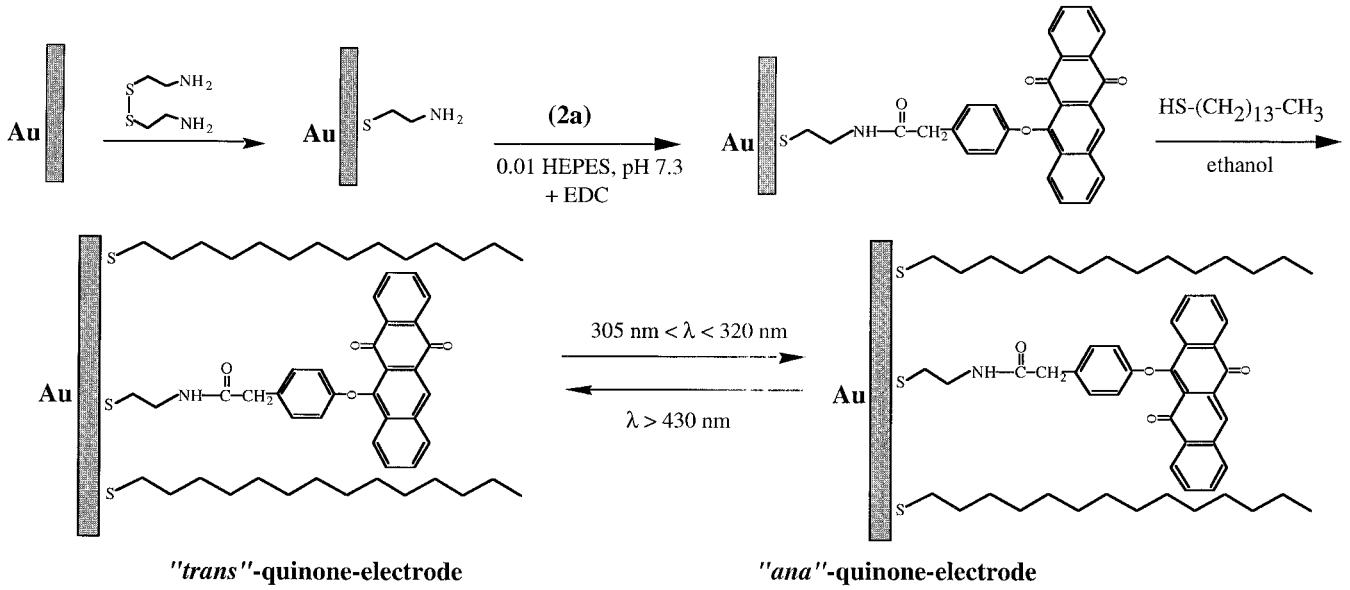

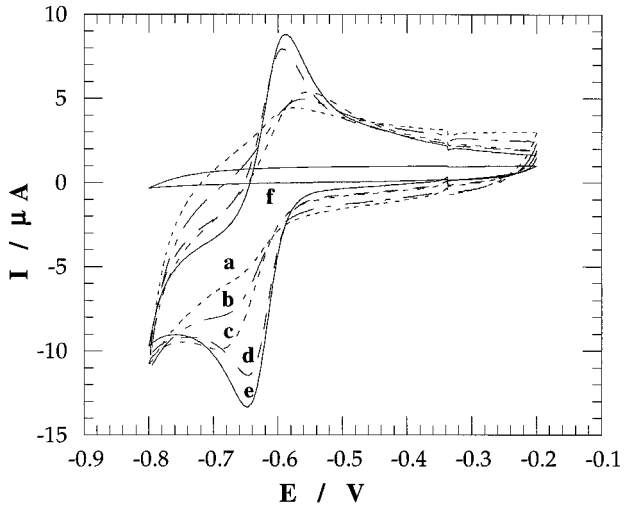

Figure 1. Cyclic voltammograms of the *trans*-quinone monolayer electrode at different time intervals of treatment with long-alkyl mercaptan C_{14}SH, (1 mM in ethanol): (a) before treatment: (b), (c), (d), and (e) 1, 4, 10, and 30 min of treatment, respectively; (f) cyclic voltammogram of an Au electrode modified with C_{14}SH only (1 mM, 30 min). Background: 0.01 M phosphate buffer, pH 7.0, and 0.1 Na_2SO_4; potential scan rate, 50 mV s^{-1}.

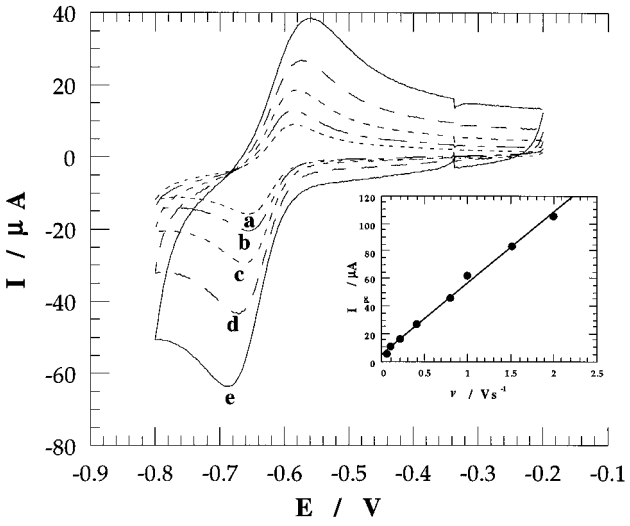

Figure 2. Cyclic voltammograms of the *trans*-quinone monolayer electrode rigidified with C_{14}SH at different potential scan rates: (a), (b), (c), (d), and (e) 0.05, 0.1, 0.2, 0.4, and 0.8 V s^{-1}, respectively. Background: 0.01 M phosphate buffer, pH 7.0, and 0.1 M Na_2SO_4. Inset: dependence of peak currents vs potential scan rate.

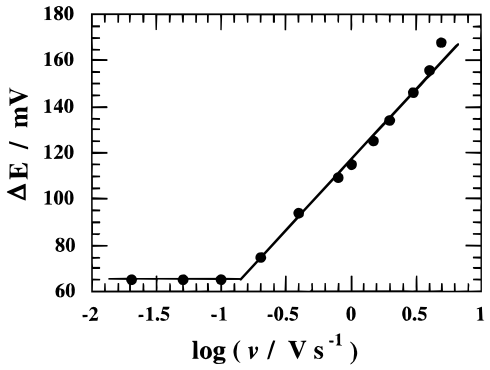

Figure 3. Dependence of the peak-to-peak separation ΔE on the potential scan rate of the *trans*-quinone/C_{14}SH mixed monolayer electrode.

rate constant to the surface-associated *trans*-quinone units is calculated to be $k_{et} \approx 2.5\ s^{-1}$. This value is close to the electron transfer rate constants of other quinones assembled as monolayers on Au electrodes.[29] Figure 4 shows the cyclic voltammograms of the *trans*-quinone/C_{14}SH mixed monolayer electrode at different pH values. The redox potential of the quinone is negatively shifted as the pH of the electrolyte increases. The redox potentials of the *trans*-quinone units correlate linearly with the pH. The slope of the E° vs pH is ca. 56.2 mV pH^{-1} (Figure 4, inset), consistent with a two-electron and two-proton electrochemical process characteristic of quinones.[33]

Figure 5 shows the cyclic voltammogram of the *trans*-quinone monolayer (curve a) and the resulting cyclic voltammogram of the *ana*-quinone monolayer electrode formed upon irradiation (305 nm < λ < 320 nm) (curve b). Thus, photoisomerization of the *trans*-quinone monolayer electrode results in the formation of the *ana*-quinone monolayer that lacks an electrochemical response. Further irradiation of the *ana*-quinone monolayer (λ > 430 nm) restores the *trans*-quinone monolayer and its

(33) Degrand, C. *Ann. Chim.* **1985**, *75*, 1.

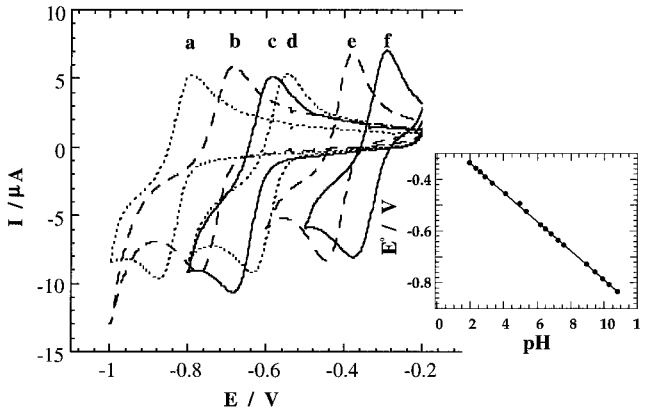

Figure 4. Cyclic voltammograms of the *trans*-quinone/C_{14}SH mixed monolayer electrode at different pH values: (a), (b), (c), (d), (e), and (f) correspond to pH values of 10.82, 8.93, 7.27, 6.48, 3.32, and 1.93, respectively. Background: 0.05 M Britton−Robinson buffer titrated to the required pH value directly in the cell; potential scan rate, 50 mV s^{-1}. Inset: E° vs pH dependence.

Scheme 3. Photoswitchable Electrocatalytic Reduction of an Electron Acceptor at the Phenoxynaphthacenequinone/C_{14}SH Mixed Monolayer Electrode Interface

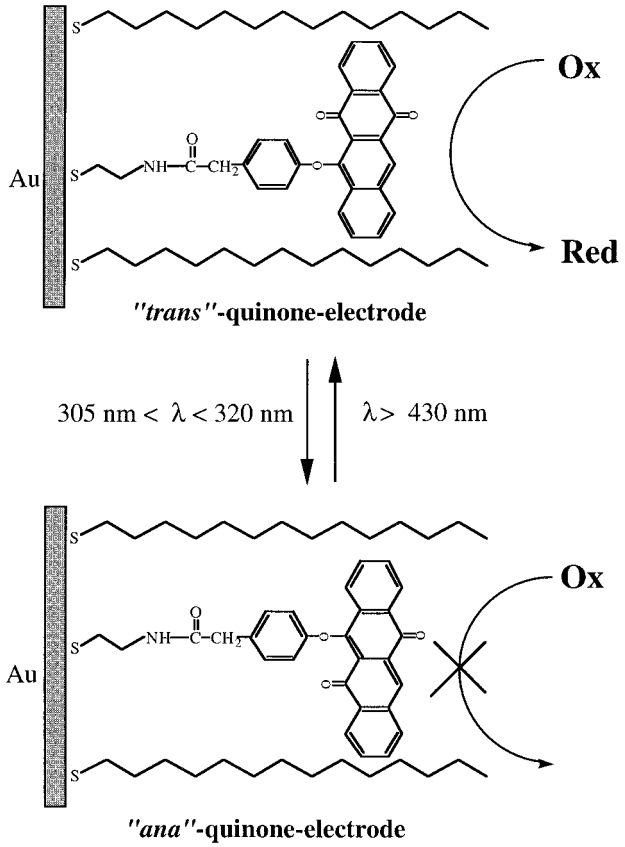

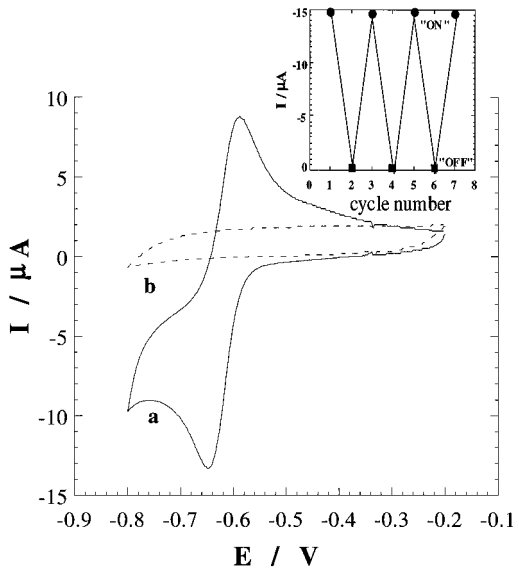

Figure 5. Cyclic voltammograms of the quinone/C_{14}SH mixed monolayer electrode in the different isomeric states produced by 1 min of irradiation with the corresponding light source: (a) *trans*-quinone, $\lambda > 430$ nm; (b) *ana*-quinone, 305 nm $< \lambda <$ 320 nm. Background: 0.01 M phosphate buffer, pH 7.0, and 0.1 M Na_2SO_4; potential scan rate, 50 mV s^{-1}. Inset: cyclic variations of peak currents of the electrode upon reversible transformation of the quinone from *trans*-state to *ana*-state, respectively. Peak currents are derived by subtraction of the capacitive current from the observed peak currents.

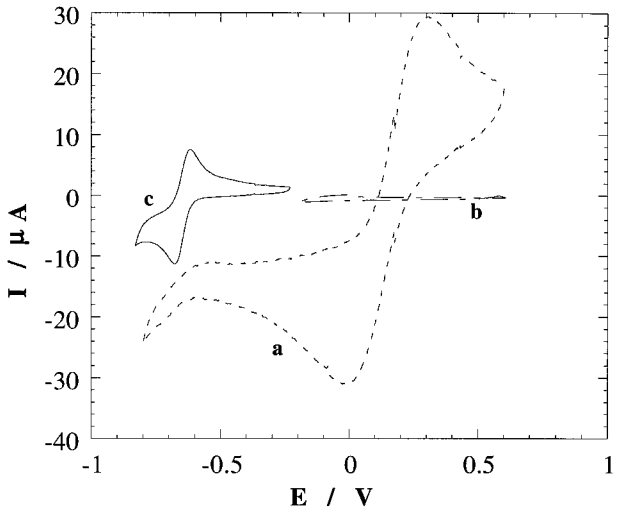

Figure 6. Cyclic voltammograms of (a) *trans*-quinone monolayer electrode in a nondensely-packed configuration in the presence of $K_3[Fe(CN)_6]$ (1×10^{-3} M), (b) *trans*-quinone/C_{14}SH mixed monolayer electrode in the presence of $K_3[Fe(CN)_6]$ (1×10^{-3} M), and (c) *trans*-quinone/C_{14}SH mixed monolayer electrode in the absence of $K_3[Fe(CN)_6]$. Background: 0.01 M phosphate buffer, pH 7.5, and 0.1 M Na_2SO_4; potential scan rate, 50 mV s^{-1}.

characteristic redox wave, as shown in Figure 5 (curve a), is regenerated. By cyclic photoisomerization of the monolayer electrode between the *trans*-quinone and *ana*-quinone states, reversible high-amperometric and zero-amperometric responses of the monolayer electrode are observed. The complete conversion (100%) from one isomer to another, which was never observed for the quinone molecules in solution, was achieved for the monolayer.[34] Thus, photochemical isomerization of the *ana*-quinone monolayer electrode into the *trans*-quinone state enables the amperometric transduction of the recorded optical signals (see inset, Figure 5). The photoisomerizable monolayer electrode represents the fundamental feature of a molecular optoelectronic device as it allows the amperometric transduction (read function) of optical signals recorded by the monolayer (write function).

Further improvement of this molecular optoelectronic system is possible by introducing a route for the amplification of the transduced signal. Scheme 3 outlines schematically the mech-

(34) The full photochemical conversion of the *trans*-quinone monolayer to the *ana*-quinone monolayer was further confirmed by the reaction of the latter monolayer with butylamine. This reaction leads to the nucleophilic substitution of the *ana*-quinone and its dissociation from the monolayer assembly. When the *ana*-quinone monolayer was reacted with butylamine in ethanol (1×10^{-3} M) for 30 min, no *trans*-quinone was detected in the monolayer upon back photoisomerization.

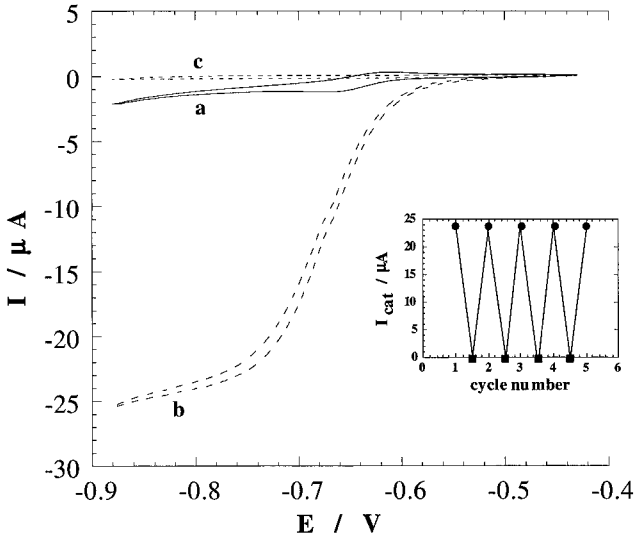

Figure 7. Cyclic voltammograms of the quinone/C_{14}SH mixed monolayer modified electrode: (a) *trans*-quinone vs the background solution; (b) *trans*-quinone in the presence of $K_3[Fe(CN)_6]$ (1×10^{-3} M); (c) *ana*-quinone in the presence of $K_3[Fe(CN)_6]$ (1×10^{-3} M). Background: 0.01 M phosphate buffer, pH 7.5, and 0.1 M Na_2SO_4; potential scan rate, 5 mV s^{-1}. Inset: cyclic variations of the electrocatalytic currents upon reversible photochemical transformation of the quinone from the *trans*-state to the *ana*-state and back. Electrocatalytic currents correspond to the current difference of the system in the presence and absence of the substrate, respectively.

Scheme 4. Light-Triggered and pH-Controlled Electrocatalytic Processes at Phenoxynaphthacenequinone/C_{14}SH Mixed Monolayer Au Electrode

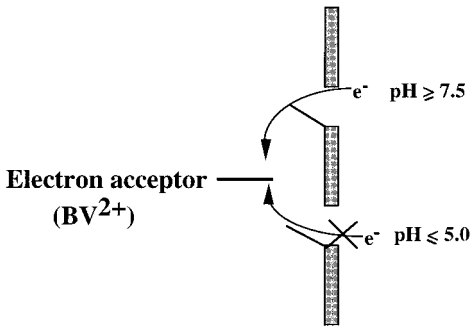

anism for the application of the *trans*-quinone/C_{14}SH mixed monolayer electrode for the amplified amperometric transduction of recorded optical signals. The *trans*-quinone monolayer acts as an electrocatalyst for the reduction of a substrate in the electrolyte, and the resulting electrocatalytic cathodic current represents an amplified transduction of the recorded optical signal. We applied two substrates, potassium ferricyanide ($Fe(CN)_6^{3-}$) and *N*,*N*′-dibenzyl-4,4′-bipyridinium (benzyl viologen) as oxidants for the reduced *trans*-quinone formed at the monolayer interface. Figure 6 (curve a) shows the cyclic voltammogram of the *trans*-quinone monolayer modified electrode prior to its treatment with C_{14}SH in the presence of ferricyanide. The quasi-reversible redox wave of $Fe(CN)_6^{3-}$/$Fe(CN)_6^{4-}$ at E° = ca. 0.14 V is observed. This indicates that direct electrical communication between $Fe(CN)_6^{3-}$ and the electrode exists simply because of the monolayer permeability. This is consistent with our previous conclusion that the *trans*-quinone monolayer assembled on the electrode is a nondensely-packed system. As a result, the electrical contact of $Fe(CN)_6^{3-}$ with the electrode originates from pinhole defects in the monolayer structure. Figure 6 (curve b) shows the cyclic voltammogram of the *trans*-quinone monolayer electrode after

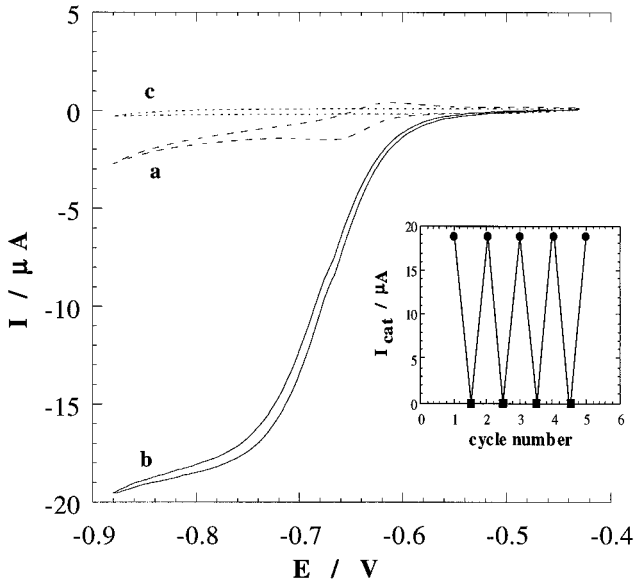

Figure 8. Cyclic voltammograms of the quinone/C_{14}SH mixed monolayer electrode: (a) *trans*-quinone vs the background solution only; (b) *trans*-quinone in the presence of benzyl viologen (BV^{2+}, 1×10^{-3} M); (c) *ana*-quinone in the presence of benzyl viologen (BV^{2+}, 1×10^{-3} M). Background: 0.01 M phosphate buffer, pH 7.5, and 0.1 M Na_2SO_4; potential scan rate, 5 mV s^{-1}. Inset: cyclic variations of the electrocatalytic currents upon reversible photochemical transformation of the quinone from the *trans*-state to the *ana*-state and back. Electrocatalytic currents correspond to the current difference of the system in the presence and absence of the substrate, respectively.

treatment with C_{14}SH and in the presence of $Fe(CN)_6^{3-}$. The redox wave of $Fe(CN)_6^{3-}$ is completely depleted, indicating that the densely-packed *trans*-quinone/C_{14}SH monolayer introduces a barrier for direct electrical communication of $Fe(CN)_6^{3-}$ with the electrode interface. Figure 6 (curve c) shows the cyclic voltammogram of the *trans*-quinone/C_{14}SH monolayer electrode in the absence of $Fe(CN)_6^{3-}$. This redox wave was discussed before and is shown here to indicate that the reduced *trans*-hydroquinone is thermodynamically capable of reducing $Fe(CN)_6^{3-}$ solubilized in the electrolyte. This discussion also implies that the *trans*-quinone/C_{14}SH monolayer electrode in the presence of $Fe(CN)_6^{3-}$ exhibits the basic features of using the system for the amplification of transduced current (Scheme 3). The monolayer assembly introduces a barrier for electroreduction of $Fe(CN)_6^{3-}$, but the electroactive *trans*-hydroquinone formed in the monolayer is capable of reducing $Fe(CN)_6^{3-}$ via a mediated electron transfer pathway. Figure 7 (curves a and b) shows the cyclic voltammograms of the *trans*-quinone/C_{14}-SH monolayer electrode in the absence and presence of $Fe(CN)_6^{3-}$, respectively. With $Fe(CN)_6^{3-}$, a high electrocatalytic cathodic current is observed, indicating that the *trans*-hydroquinone catalyzes the reduction of $Fe(CN)_6^{3-}$. Photochemical isomerization of the monolayer to the *ana*-quinone state (305 nm < λ < 320 nm) blocks the electrochemical reduction of $Fe(CN)_6^{3-}$. Since the *ana*-quinone is electrochemically inactive in this potential range, the mediated reduction of $Fe(CN)_6^{3-}$ is inhibited. Further irradiation of the *ana*-quinone monolayer (λ > 430 nm) restores the *trans*-quinone monolayer, and the electrocatalytic reduction of $Fe(CN)_6^{3-}$ is reactivated. By cyclic photoisomerization of the monolayer electrode between the *trans*-quinone/C_{14}SH and *ana*-quinone/C_{14}SH states, the reversible amplified amperometric transduction of the recorded optical signals can be reversibly switched "on" and "off", respectively (see inset, Figure 7).

One should recall, however, that the redox potential of the *trans*-quinone component in the monolayer assembly is pH-

Scheme 5. Bioelectrocatalyzed Reduction of Nitrate using the Photoisomerizable Quinone/C_{14}SH Monolayer Electrode and a Vectorial Electron Transfer Cascade (NR = nitrate reductase)

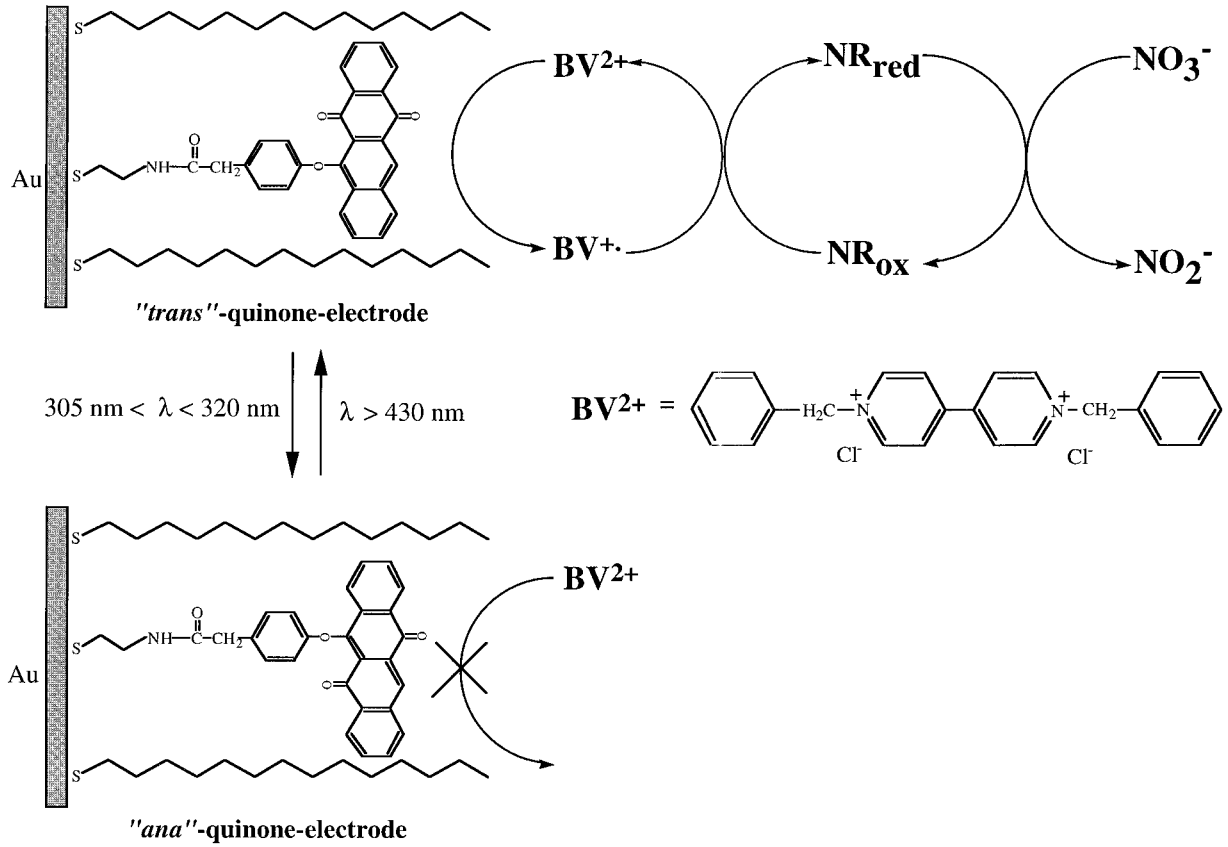

dependent. By the selection of a redox probe in the electrolyte solution exhibiting a reduction potential close to that of the reduction potential of the *trans*-quinone component, the electrocatalyzed reduction of the redox probe and, consequently, the resulting electrocatalytic cathodic current could be controlled by two parameters: the photoisomer state of the monolayer and the pH of the electrolyte solution. *N,N*′-Dibenzyl-4,4′-bipyridinium (BV^{2+}) exhibits a pH-independent reduction potential corresponding to $E^\circ = -0.58$ V.[35] The formal potentials of the *trans*-hydroquinone in the monolayer assembly are $E^\circ = -0.65$ V at pH = 7.5 and $E^\circ = -0.51$ V at pH = 5.0, respectively. Thus, at pH = 7.5 the hydroquinone should be thermodynamically capable of inducing the vectorial electrocatalytic reduction of BV^{2+}, while at pH = 5.0 the electrocatalytic reduction of BV^{2+} should be blocked (Scheme 4). The redox responses of the photoisomerizable *trans*-quinone/C_{14}-SH mixed monolayer electrode were examined in the presence of BV^{2+}. Figure 8 shows the cyclic voltammogram of the *trans*-quinone monolayer at pH = 7.5 in the absence (curve a) and presence (curve b) of BV^{2+}. In the presence of BV^{2+}, a high electrocatalytic cathodic current is observed, indicating that the *trans*-hydroquinone catalyzes the reduction of BV^{2+}. Knowing the concentration of BV^{2+}, its diffusion coefficient[35] $D = 0.43 \times 10^{-5}$ cm^2 s^{-1}, and the electrocatalyst surface density and using the experimental electrocatalytic cathodic current, the second-order electron transfer rate constant from *trans*-hydroquinone to BV^{2+} was calculated to be $k_{et} \approx 5 \times 10^4$ M^{-1} s^{-1}. Photoisomerization of the monolayer (305 nm < λ < 320 nm) results in the formation of the electrochemically inactive *ana*-quinone monolayer, and the electrocatalyzed reduction of BV^{2+} is blocked (Figure 8, curve c). By further light-induced isomerization of the monolayer (λ > 430 nm), the *trans*-quinone monolayer is regenerated and the electrocatalytic anodic current corresponding to the reduction of BV^{2+} is restored. Cyclic photoisomerization of the monolayer between the *trans*-quinone and *ana*-quinone states allows the reversible amplified transduction of the recorded optical signals (inset, Figure 8). When the pH of the electrolyte solution was altered to pH = 5.0, the electrochemical response of the *trans*-quinone/C_{14}SH monolayer is positively shifted by ca. 140 mV ($E^\circ = -0.5$l V). Addition of BV^{2+} to the electrolyte solution does not yield any electrocatalytic cathodic current. This is consistent with the fact that the vectorial, mediated reduction of BV^{2+} ($E^\circ = -0.58$ V) is thermodynamically not feasible by the *trans*-hydroquinone at pH = 5.0. The photoswitchable electrocatalytic activity of the quinone/C_{14}SH modified electrode in the presence of BV^{2+} resembles the functions of a light-triggered transistor (Scheme 4). Photoisomerization of the monolayer electrode opens or closes the electrical gate of the electrode (*trans*-quinone is "open"; *ana*-quinone is "closed"). The pH of the electrolyte solution controls the potential of the gate. At pH = 7.5 or higher pH values, the gate enables electrical contact with the electron acceptor (BV^{2+}) and the current flows through the system. At pH = 5.0 or lower, the "*trans*"-quinone opens the gate, but the electron flow is prohibited.

The presence of the electron acceptor in the electrolyte cell provides the basic means to amplify the recorded optical signal by the vectorial electron transfer stimulated by the electroactive component associated with the monolayer. The phenomenon of amplification could be further improved by the coupling of a secondary catalyst that recycles the oxidized electron acceptor at the *trans*-quinone electrode interface. Electro reduction of BV^{2+} by *trans*-hydroquinone yields the *N,N*′-dibenzyl-4,4′-bipyridinium radical cation ($BV^{+\bullet}$). Previous studies indicated that bipyridinium radical cations can mediate electron transfer

(35) Bird, C. L.; Kuhn, A. T. *Chem. Soc. Rev.* **1981**, *10*, 49.

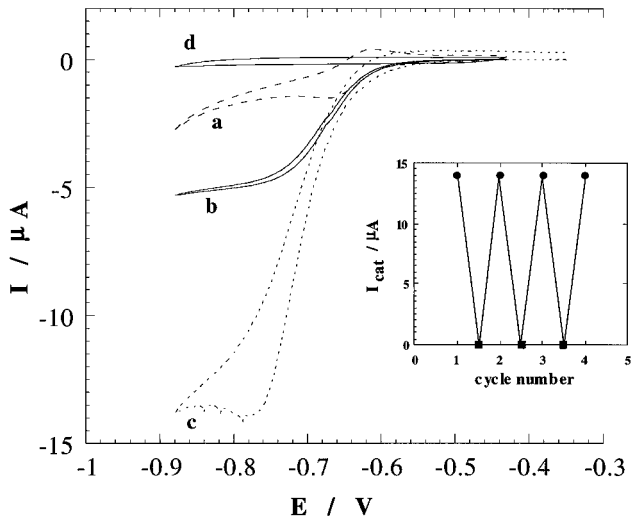

Figure 9. Cyclic voltammograms of the quinone/C_{14}SH mixed monolayer electrode: (a) *trans*-quinone vs the background solution; (b) *trans*-quinone in the presence of benzyl viologen (BV^{2+}, 3×10^{-4} M) and nitrate reductase (1 unit mL^{-1}); (c) *trans*-quinone in the presence of benzyl viologen (BV^{2+}, 3×10^{-4} M), nitrate reductase (1 unit mL^{-1}), and KNO_3 (50 mM); (d) *ana*-quinone in the presence of benzyl viologen (BV^{2+}, 3×10^{-4} M), nitrate reductase (1 unit mL^{-1}), and KNO_3 (50 mM). Background: 0.01 M phosphate buffer, pH 7.5, and 0.1 M Na_2SO_4; potential scan rate, 5 mV s^{-1}. Inset: cyclic variations of the electrocatalytic currents upon cyclic photochemical transformation of the quinone from the *trans*-state to the *ana*-state and back. Electrocatalytic currents correspond to the current difference of the system in the presence and absence of the substrate, respectively.

to redox enzymes such as nitrate reductase or glutathione reductase.[36] Thus, introduction of the enzyme nitrate reductase and its substrate (NO_3^-) would enable the $BV^{+\bullet}$-mediated bioelectrocatalyzed reduction of nitrate and the regeneration of the electron acceptor BV^{2+} at the monolayer electrode interface (Scheme 5). Thus, conjugation of the biocatalyst/substrate to BV^{2+} generates an electron transfer cascade that is anticipated to further amplify the electrical activity of the *trans*-quinone monolayer. Figure 9 shows the cyclic voltammograms of the *trans*-quinone/C_{14}SH monolayer electrode in the absence and presence of BV^{2+} (curves a and b, respectively). The amplified electrochemical activity of the quinone monolayer as a result of the reduction of BV^{2+} is observed. Addition of nitrate reductase (NR) and nitrate results in the cyclic voltammogram shown in Figure 9 (curve c). An increase in the electrocatalytic cathodic current is observed as compared to the system that includes only BV^{2+}. Thus, the electron transfer cascade, where the primary reduced acceptor drives the biocatalytic reduction of nitrate, further enhances the transduced electroactivity of the quinone monolayer. By photochemical isomerization of the *trans*-quinone monolayer to the *ana*-quinone state (305 nm < λ < 320 nm), the electron transfer cascade is blocked, and by reversible photochemical isomerization of the monolayer between the *trans*-quinone and *ana*-quinone states, cyclic activation and deactivation of the electron transfer cascade is achieved (Figure 9, curve d and inset).

One can realize that by coupling the electroactive "*trans*"-quinone monolayer to a diffusional acceptor substrate, amplification of the interfacial vectorial electron transfer is accomplished. For example, by the coupling of BV^{2+} (1×10^{-3} M) to the electroactive monolayer electrode, a ca. 10-fold enhancement in the current response is observed (Figure 8). The extent of current amplification is, however, tuned by the concentration of the acceptor substrate. In order to activate the $BV^{+\bullet}$-mediated enzyme cascade with nitrate reductase/NO_3^- as an amplification means, a relatively low concentration of BV^{2+} is employed (3×10^{-4} M). At these conditions, the current amplification by BV^{2+} is only ca. 2.5-fold, but the enzyme cascade amplifies the initial cathodic current by ca. 6.5-fold. We thus realize two alternative methods to amplify the electrochemical responses in future electronic devices. By the assembly of redox-active layers exhibiting an appropriate reduction potential gradient on a base photoelectroactive monolayer, vectorial electron transfer could lead to the gated amplification of light signals recorded by the monolayer.

Conclusions

We have tailored a photoisomerizable naphthacenequinone monolayer electrode for the amperometric transduction of recorded optical signals. A reversible electrochemical activity of the *trans*-quinone monolayer was observed only after the organization of a densely-packed, structurally-ordered monolayer assembly. By the coupling of electron acceptors to the electroactive monolayer electrode, vectorial electron transfer that yields the amplification of the recorded optical signals was accomplished. The pH-tunable potentials of the *trans*-quinone monolayer assembly allowed us to design systems in which the vectorial electron transfer is pH-controlled and photochemically-gated. The resulting systems duplicate functions of photochemically-triggered transistors at the molecular level. Finally, we demonstrated that the coupling of an electron transfer cascade to the electroactive quinone monolayer results in an enhanced amplification of the transduced amperometric signals. The various systems represent novel configurations of optomolecular electronic devices of potential applications in information storage and processing.

Acknowledgment. This research was supported by The Israel Academy of Sciences and Humanities.

JA961814B

(36) (a) Steckhan, E.; Kuwana, T. *Ber. Bunsen-Ges. Phys. Chem.* **1974**, *78*, 253. (b) Fernandez, V. M. *Anal. Biochem.* **1983**, *130*, 54. (c) Willner, I.; Lapidot, N.; Riklin, A.; Kasher, R.; Zahavy, E.; Katz, E. *J. Am. Chem. Soc.* **1994**, *116*, 1428.